

AN ABSTRACT OF THE THESIS OF

William Frank Unzicker for the M. S. in Chemical Engineering
(Name) (Degree) (Major)

Date thesis is presented 7/25/66

Title TURBULENT HEAT TRANSFER IN ANNULI AT LARGE
DIAMETER RATIOS

Abstract approved _____

Redacted for Privacy

(Major professor)

Heat transfer from the inner wall of an annulus to subcooled water in turbulent parallel flow was studied. The inner core of the annulus consisted of wires varying from 0.0019 to 0.0197 inch in diameter. The outer tube consisted of a 1.01 inch diameter glass tube 24 inches long. Diameter ratios therefore varied from 530:1 to 51:1. The water velocity varied from 1.8 to 13.5 feet per second. Rectified alternating current was supplied to the wires. The current, wire surface area, wire resistance, and bulk water temperature were measured and from this data the average convective heat transfer coefficient calculated. The heat transfer coefficient varied from 1840 to 4990 BTU/hr. ft.². F for the 0.0197 inch diameter wire to 7210 to 13000 BTU/hr. ft.². F for the 0.0019 inch diameter wire.

The data agreed well with that of Mueller who had worked with air in annuli of large diameter ratios. The data correlated when plotted as $N_{Nu}/N_{Pr_f}^{1/3}$ versus N_{Re} when the equivalent diameter was based on experimentally determined radii of maximum velocity

in turbulent annular flow. Over the range of operating conditions studied the heat transfer coefficients were considerably lower than predicted by the usual empirical equations.

TURBULENT HEAT TRANSFER IN ANNULI
AT LARGE DIAMETER RATIOS

by

WILLIAM FRANK UNZICKER

A THESIS

submitted to

OREGON STATE UNIVERSITY

in partial fulfillment of
the requirements for the
degree of

MASTER OF SCIENCE

June 1967

APPROVED:

Redacted for Privacy

Professor of Chemical Engineering

In Charge of Major

Redacted for Privacy

Head of Department of Chemical Engineering

Redacted for Privacy

Dean of Graduate School

Date thesis is presented

Typed by Marion F. Palmateer

July 25, 1966

ACKNOWLEDGMENTS

My sincere appreciation to Professor J. G. Knudsen for providing me the opportunity to do this research project. His advice and support were deeply appreciated. My gratitude is given to Professor J. R. Welty for renewing my interest in heat transfer. To Professor J. S. Walton, Head, and the staff of the Chemical Engineering Department, for their encouragement, consideration, and financial aid during the course of my studies, I will forever be indebted. To each and all of the above I give a grateful and sincere thank you.

A very special thank you to my wife for her encouragement, patience, and sacrifice without which this paper would never have been written.

TABLE OF CONTENTS

| | <u>Page</u> |
|-----------------------------------|-------------|
| INTRODUCTION | 1 |
| BACKGROUND AND THEORY | 3 |
| EXPERIMENTAL EQUIPMENT | 8 |
| Flow System | 8 |
| Electrical System | 10 |
| EXPERIMENTAL PROCEDURE | 12 |
| Test Wire Calibration | 12 |
| Test Runs | 14 |
| EXPERIMENTAL DATA | 16 |
| DISCUSSION | 24 |
| CONCLUSIONS AND RECOMMENDATIONS | 27 |
| BIBLIOGRAPHY | 28 |
| APPENDICES | 29 |
| APPENDIX I. NOMENCLATURE | 29 |
| APPENDIX II. EXPERIMENTAL DATA | 32 |
| APPENDIX III. ORIFICE CALIBRATION | 37 |
| APPENDIX IV. SAMPLE CALCULATIONS | 38 |

LIST OF FIGURES

| <u>Figure</u> | | <u>Page</u> |
|---------------------|--|-------------|
| 1 | Flow System. | 9 |
| 2 | Electrical System. | 11 |
| 3 | Correlation Based on Wire Diameter. | 17 |
| 4 | Correlation Based on Wire and Tube Diameters. | 18 |
| 5 | Correlation Based on Wire Diameter and Fluctuating Radial Velocity. | 19 |
| 6 | Correlation Based on Film Conditions and Equivalent Diameter for Turbulent Flow. | 20 |
| 7 | Correlation Based on Film Conditions and Equivalent Diameter for Laminar Flow. | 21 |
| 8 | Correlation Based on Film Conditions and Equivalent Diameter for Turbulent Flow. | 22 |
| <u>Appendix</u> | | |
| <u>Figure</u> | | |
| 1 | Orifice Calibration. | 37 |

LIST OF TABLES

| <u>Table</u> | | <u>Page</u> |
|-----------------|--|-------------|
| 1 | Predicted and measured heat transfer coefficients for 0.0019 inch diameter wire | 16 |
| <u>Appendix</u> | | |
| <u>Table</u> | | |
| 1 | Summary of experimental data, 0.0019 inch wire | 32 |
| 2 | Summary of experimental data, 0.0044 inch wire | 32 |
| 3 | Summary of experimental data, 0.0095 inch wire | 33 |
| 4 | Summary of experimental data, 0.012 inch wire | 34 |
| 5 | Summary of experimental data, 0.0159 inch wire | 35 |
| 6 | Summary of experimental data, 0.0197 inch wire | 36 |

TURBULENT HEAT TRANSFER IN ANNULI AT LARGE DIAMETER RATIOS

INTRODUCTION

Present methods of correlating turbulent heat transfer coefficients for the inner wall of an annulus show considerable deviation from experimental data when applied to annuli of large outer to inner diameter ratio. Nolan (10) showed that predicted values of the coefficient exceeded the estimated value obtained from his experimental data by a factor ranging from five to ten. The probable reason for the discrepancies is that present correlations are based on experimental data covering annuli with diameter ratios up to about 20. Present relationships place too great an emphasis on diameter ratio so that, at large diameter ratios, extremely large values of the heat transfer coefficient are predicted. The work of Mueller (9) appears to be the only published data involving diameter ratios greater than 20. In his work, Mueller used ratios ranging from 760 to 6900.

The present study was performed to measure non-boiling heat transfer coefficients for the inner wall of an annulus with diameter ratios ranging from 50 to 500. From this work, it was hoped that new knowledge could be obtained which would permit accurate prediction of heat transfer coefficients in annuli of diameter ratios from one (parallel planes) to infinity (circular pipes).

In this work, the annulus consisted of a fine nickel wire located concentrically in a one inch diameter tube. Six wire sizes were used, ranging from 0.0019-inch diameter to 0.0197-inch diameter. Heat transfer was to subcooled water flowing at velocities ranging from 1.8 to 13.5 feet per second.

BACKGROUND AND THEORY

Since publication of the Colburn analogy (2), considerable effort has been expended by many investigators to correlate annular heat transfer data using the j -factor for heat transfer. A commonly used equation is of the form

$$j_{h_1} = C N_{Re_{de}}^{-0.2} \left(\frac{d_1}{d_2} \right)^{-n}$$

Wiegand (12) gives values of 0.023 and 0.45 for C and n respectively, while Monrad and Pelton (8) assign values of 0.020 and 0.53 to the same constants. McAdams (7) recommends the above equation with C equal to 0.023 and $\left[\frac{\mu_b}{\mu_w} \right]^{0.14}$ substituted for the diameter ratio for heat transfer from both the inner and outer walls of concentric annuli.

A special form of the Colburn analogy between heat and momentum transfer was proposed by Knudsen (3). Special consideration was given to the effect of shear stresses at the walls. The j -factor for heat transfer was defined in the usual way.

$$j_h = \left[\frac{h}{C_p G} \right] \left[\frac{C_p \mu}{k} \right]^{2/3} = \frac{f}{2}$$

Since the friction factor for annuli differs from that for pipes,

Knudsen suggested that the friction factor for the inner wall of an annulus is

$$\frac{f}{2} = 0.023 N_{Re_{de}}^{-0.2} \left[\frac{1-A}{1-\lambda^2} \right]^{0.2} \frac{\lambda^2 - A^2}{A(1-\lambda^2)}$$

Combining these two relationships one obtains

$$j_{h_1} = \left[\frac{h}{C_p G} \right] \left[\frac{C_p \mu}{k} \right]^{2/3} = 0.023 N_{Re_{de}} \left[\frac{1-A}{1-\lambda^2} \right]^{0.2} \frac{\lambda^2 - A^2}{A(1-\lambda^2)}$$

from which it is possible to predict heat transfer coefficients knowing fluid properties, the mass flow rate, and the geometry of the system.

A commonly used method of describing the geometry of the system is to use an equivalent diameter defined by four times the cross sectional flow area divided by the wetted perimeter. For annuli, this definition reduces to $d_2 - d_1$, which is the equivalent diameter used by Wiegand (12), Monrad and Pelton (8), and Knudsen (3). However, at large diameter ratios, $d_2 - d_1$ approaches d_2 so that the geometry of the system is not adequately described particularly when heat transfer is from the inner tube. Even with small diameter ratios, Wiegand and Monrad and Pelton found it necessary to use a diameter ratio to correlate data.

As a result of his study involving shear stresses at the wall, Knudsen (3) included a factor λ which is defined as the ratio of the

radius of maximum velocity to the radius of the outer tube.

It is also possible to define an equivalent diameter based on the radius of maximum velocity.

$$d_{em} = 2r_1 \left[\left(\frac{r_m}{r_1} \right)^2 - 1 \right]$$

The problem which arises with this relationship is the determination of the point of maximum velocity. Rothfus et al (11) showed experimentally that, for turbulent flow in annuli,

$$r_m^2 = \frac{r_2^2 - r_1^2}{2 \ln \left(\frac{r_2}{r_1} \right)}$$

which is the same relationship which may be derived analytically for laminar flow (4).

More recent experimental data by Brighton and Jones (1) indicate that the point of maximum velocity for turbulent flow is closer to the inner wall than for laminar flow. While the difference is small in annuli of small diameter ratios, a very significant difference occurs at large diameter ratios. The data of Brighton and Jones substantiates the determination of the point of maximum velocity predicted analytically by Macagno and McDougall (6).

When heat is transferred from a small diameter inner core of an annulus (high diameter ratios) to a fluid in turbulent motion, the

mechanism of heat transfer may be different from heat transfer from the inner surface of concentric pipes (i. e. at low diameter ratios).

Turbulent flow is characterized by a random motion of fluid particles. This random motion produces eddies which may have instantaneous velocities in any direction. The instantaneous velocity in one direction is the sum of the time averaged, or bulk motion in the same direction, and a fluctuating velocity component, the magnitude of which depends upon the intensity of turbulence. If no bulk flow occurs in the x direction, this would mean only that the average fluctuating velocity in the x direction is zero but would not rule out velocities in the positive x and negative x direction. It is conceivable, in turbulent flow parallel to the axis of an annulus containing a fine wire, that eddies with radial velocity fluctuations are large compared to the wire diameter so that, in the vicinity of the wire, the effects of the bulk fluid flow are not significant.

If this proposition is valid, it should be possible to correlate heat transfer data from annuli containing fine wires by an empirical equation used for fluid flow transverse to a cylinder if one has a knowledge of the magnitude of the fluctuating radial velocity. The equation recommended by McAdams (7) is

$$\frac{hd_1}{k} \left(\frac{C_p \mu}{k} \right)^{0.3} = 0.35 \sqrt{0.56 \left[\frac{\rho d_1 v'}{\mu} \right]^{0.52}}$$

where v' is the fluctuating radial cross velocity.

Mueller (9) measured the heat transfer from wires to air and found his data correlated best when $N_{Nu_1} (d_2)^{-0.2}$ was plotted versus N_{Re_1} . His data were about 40 percent lower than predicted by McAdams' (7) for air flow normal to a single cylinder.

EXPERIMENTAL EQUIPMENT

Flow System

The flow system is shown schematically in Figure 1. Details of the system were reported by Nolan (10).

The test section consisted of a precision bored glass tube with an inside diameter of 1.01 inches and a length of 24 inches. The test wire ran concentrically along the length of the glass tube and was attached to one-eighth inch copper or brass leads which extended through seals at the top of the vertical test section and bottom of the entrance pipe.

A 48 inch length of pipe preceded the test section in an effort to assure a fully developed velocity profile in the test section.

Demineralized water, produced from steam condensate, was recirculated through the test section by pumping from a jacketed 20 gallon stainless steel tank. Cooling water passed through the jacket during test runs while cooling water or steam was circulated through the jacket when the test wire was calibrated.

The flow rate was measured by a calibrated sharp-edged orifice. Radius taps were used to measure the pressure drop across the orifice. The pressure taps were connected to a manometer containing carbon tetrachloride under water.

Oil-filled thermometer wells were installed before the entrance

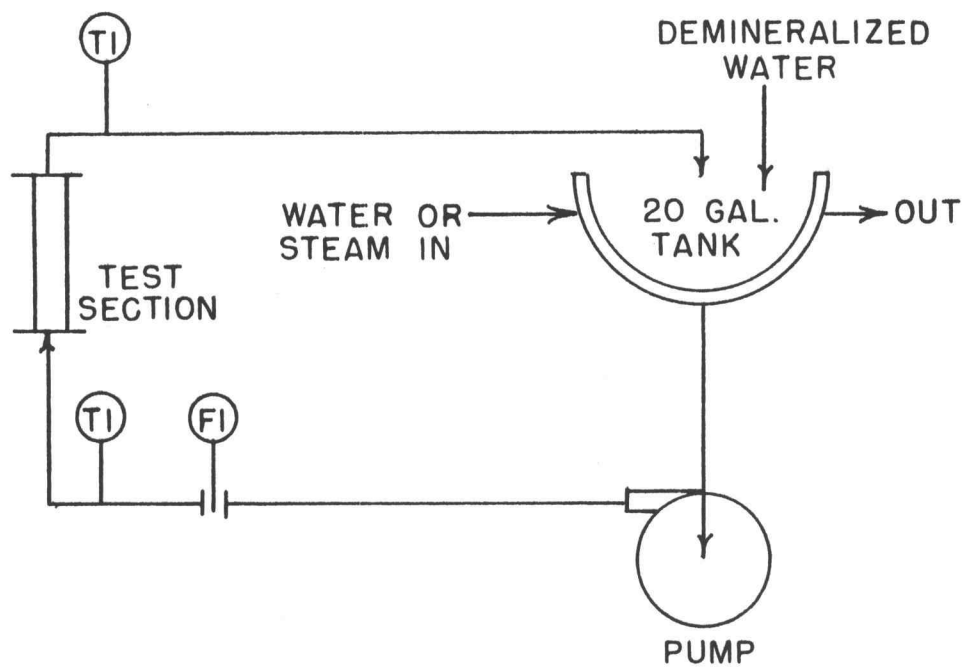


Figure 1. Flow System.

length and after the test section to measure the bulk water temperature. The mercury-filled thermometers used covered a range of 30 to 220° divided into one-fifth degree increments.

Electrical System

The electrical system is shown schematically in Figure 2.

Direct current was supplied to the test wire rather than alternating current because only D. C. potentiometers were available. The direct current was provided by a copper oxide rectifier operating off a 220 volt, three phase A. C. supply. The current passed through a calibrated 20 ampere manganin shunt resistance, R_I , submerged in an oil bath, the test wire, R_w , and then to the ground.

A high resistance shunt, R_{ws} , was installed in parallel with the test wire. The shunt consisted of two calibrated resistors and was required to permit measurement of voltages which exceeded the potentiometer range. By measuring the voltage across the smaller resistance and knowing the total shunt resistance, it was possible to calculate the total voltage across the shunt. The total voltage across the shunt was equal to the voltage across the test wire and leads.

The test wire calibration circuit consisted of a two volt storage battery, a variable resistor, R_v , and a standard one ohm (± 0.002 percent) resistor, R_s , in series with the test wire.

Voltage measurements were made with a Leeds and Northrup K-2 potentiometer.

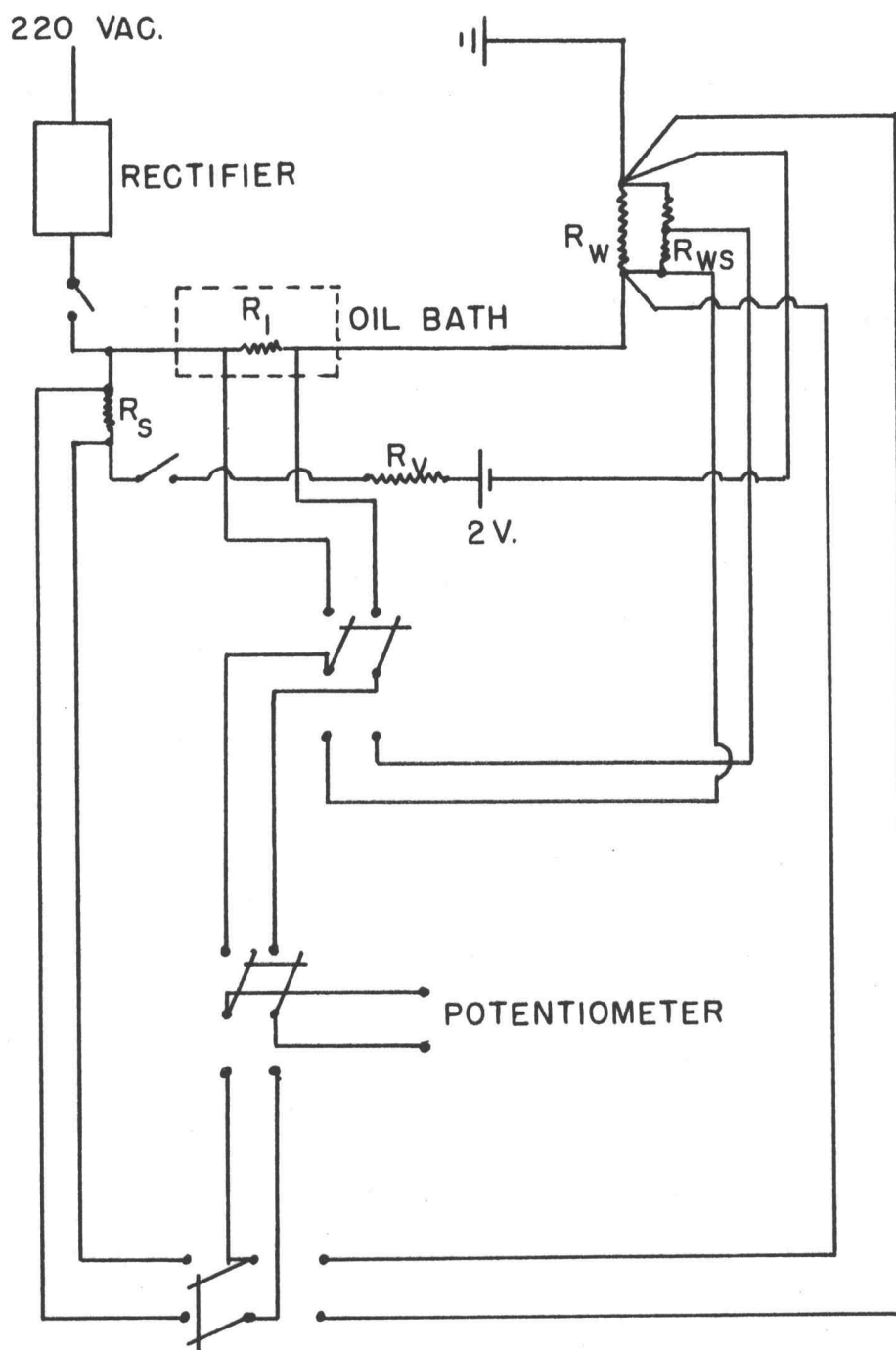


Figure 2. Electrical System.

EXPERIMENTAL PROCEDURE

Test Wire Calibration

Nickel wire was used in all tests. The diameter of the test wire was measured to 0.0001 inch at a number of points along its length using a micrometer and the average diameter used in calculating wire surface area.

The test wire was inserted into holes drilled in the tips of the leads and silver soldered. The lead tips were streamlined using a file and emery cloth. The length of the test wire was then measured to one-sixteenth inch.

The leads and test wire were installed in the test equipment with the leads extending about three-fourths inch into the test section. Power and electrical measurement leads were attached to the ends of the leads which extended beyond the seals of the test section and entrance pipe. Considerable care was exercised in drawing the test wire taut without stretching or kinking it.

Demineralized water was added to the holding tank and was recirculated through the test section. Manometer lines were flushed with water to remove any entrapped air.

Cooling water or steam was circulated through the holding tank

jacket to maintain the tank contents at a constant temperature. A slight ($\pm 0.3^\circ\text{F}$) change in the bulk water temperature between the inlet and outlet thermometers was observed. The average of the inlet and outlet water temperatures was considered the bulk temperature and the wire temperature during calibration.

When the bulk water temperature remained constant for 15-20 minutes, 0.002-0.006 amperes were passed through the test wire from the two volt storage battery. The low current was used in an effort to prevent the test wire temperature from exceeding the bulk water temperature by any significant amount. With the measured heat transfer coefficients, the calculated wire temperature was less than 0.01°F above the bulk water temperature.

The galvanometer was zeroed and the potentiometer standardized. Three or four voltage measurements were made alternately across the standard resistor and the test wire and leads. Since the standard resistor had a resistance of one ohm ± 0.00002 ohms, the measured voltage across the standard resistor was considered equal to the number of amperes passing. Dividing the voltage across the test wire and leads by the current gave the resistance of the test wire and leads.

After obtaining satisfactory agreement between resistance measurements at one temperature, the bulk water temperature was adjusted to a new value and the calibration procedure repeated.

At least two calibrations were made on each wire to ensure reproducibility of the data.

The average resistance of the leads was determined in a similar manner and was subtracted from the resistance measured in the test runs prior to calculating the power generated in the wire.

Test Runs

Cooling water was circulated through the holding tank jacket to maintain the bulk water temperature at 65-75°F and the oil bath temperature was adjusted to 30-35°C by turning on the oil recirculation pump. The rectifier was turned on and the water flow through the test section adjusted to the desired rate. Fifteen to thirty minutes were allowed to permit the system to come to equilibrium.

Normally ten sets of voltage measurements were made at each flow rate. Each set of measurements consisted of the voltage across the 20 ampere shunt to measure current and the voltage across the smaller of the two test wire shunt resistors. Ten sets of readings were taken because of the variation in potentiometer readings due probably to fluctuations in supply line voltage. At times, normally weekends or late evening, very good precision was achieved between potentiometer readings, so that only five sets of measurements were taken.

After readings were taken at one flow rate, the flow rate was

adjusted to a new value. Fifteen to thirty minutes were allowed between readings taken at different flow rates to permit the system to reach equilibrium.

Data were taken at four to six flow rates ranging from about one to six pounds mass per second. Tests were made with wires with nominal diameters of 0.002, 0.005, 0.010, 0.012, 0.016, and 0.020 inch. One to three runs were made with each wire size, with a new wire used for each run.

No adjustment was made in the power output from the rectifier. The power output was determined by the external resistance which in this case is the test wire.

EXPERIMENTAL DATA

Predicted and measured heat transfer coefficients for 0.0019 inch diameter wire are presented in Table 1. Summaries of the experimental data are presented in Appendix Table 1 through 6. Graphical correlations of the data are presented in Figures 3 through 8. In these figures N_{Pr} is evaluated at film conditions. N_{Nu} and N_{Re} are evaluated at bulk conditions unless stated otherwise.

Table 1. Predicted and measured heat transfer coefficients for 0.0019 inch diameter wire

| Flow Rate LBM hr. ft. ² | Heat Transfer Coefficients BTU/hr. ft. ² • F | | | |
|--|---|---------|----------------------|---------|
| | Measured | Wiegand | Monrad and Pelton | Knudsen |
| 6.48×10^5 | 7200 | 10300 | 14300 | 34000 |
| 1.425×10^6 | 9190 | 13300 | 17000 | 39800 |
| 2.27×10^6 | 11200 | 21700 | 24900 | 65000 |
| 2.78×10^6 | 11700 | 36200 | 46300 | 108000 |
| 3.30×10^6 | 12400 | 41800 | 52700 | 125000 |
| 3.76×10^6 | 13000 | 45000 | 57400 | 135000 |

In Figure 3, the data are correlated by plotting $N_{Nu}/N_{Pr}^{1/3}$ versus N_{Re_1} .

In Figure 4, $N_{Nu_1}/N_{Pr}^{1/3} D_2^{0.2}$ is plotted versus N_{Re_1} . The results by Mueller (9) on heat transfer from wires to air are also presented.

Figure 5 shows the results when $N_{Nu_1}/N_{Pr}^{1/3}$ is plotted versus

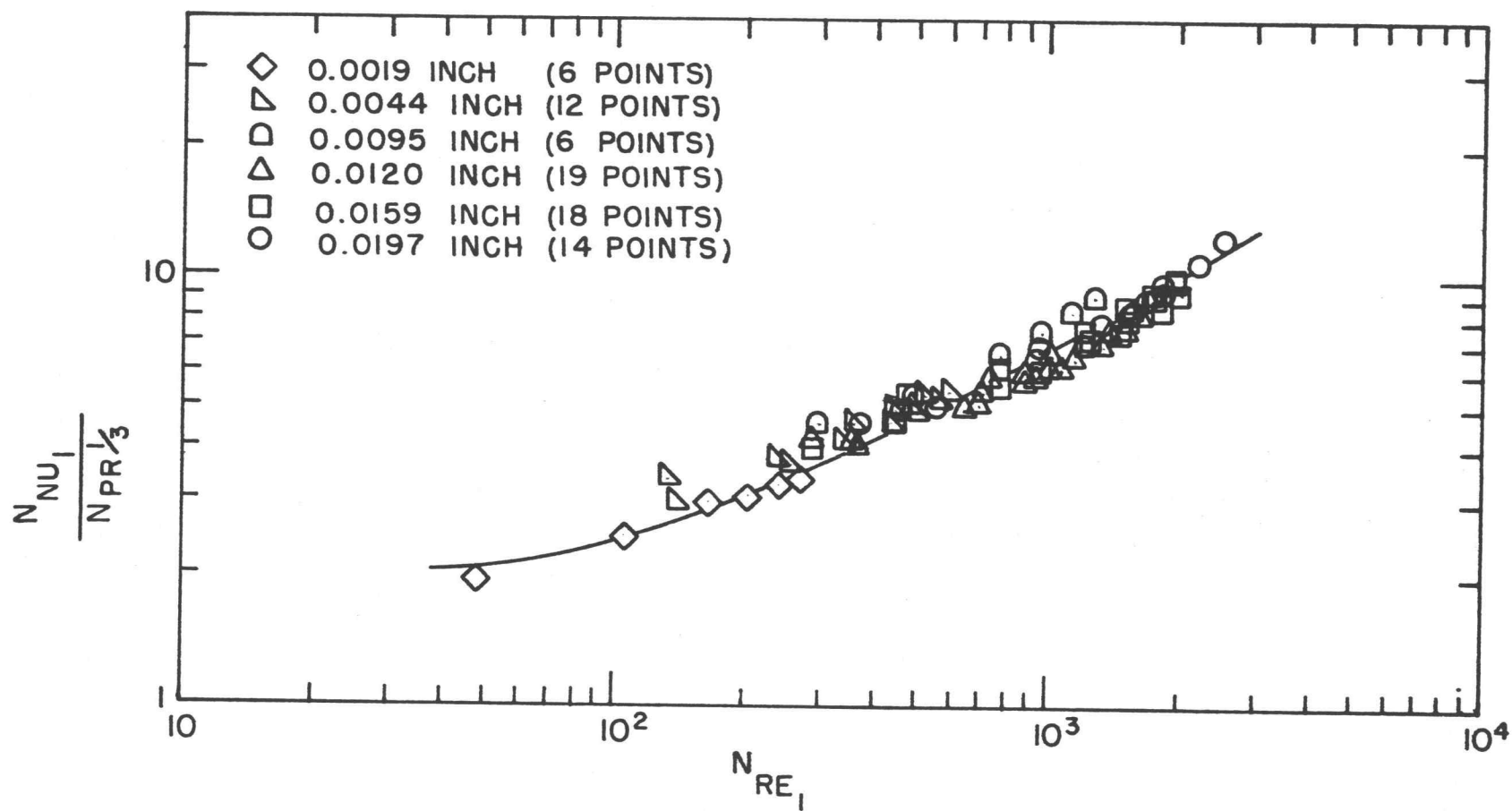


Figure 3. Correlation Based On Wire Diameter.

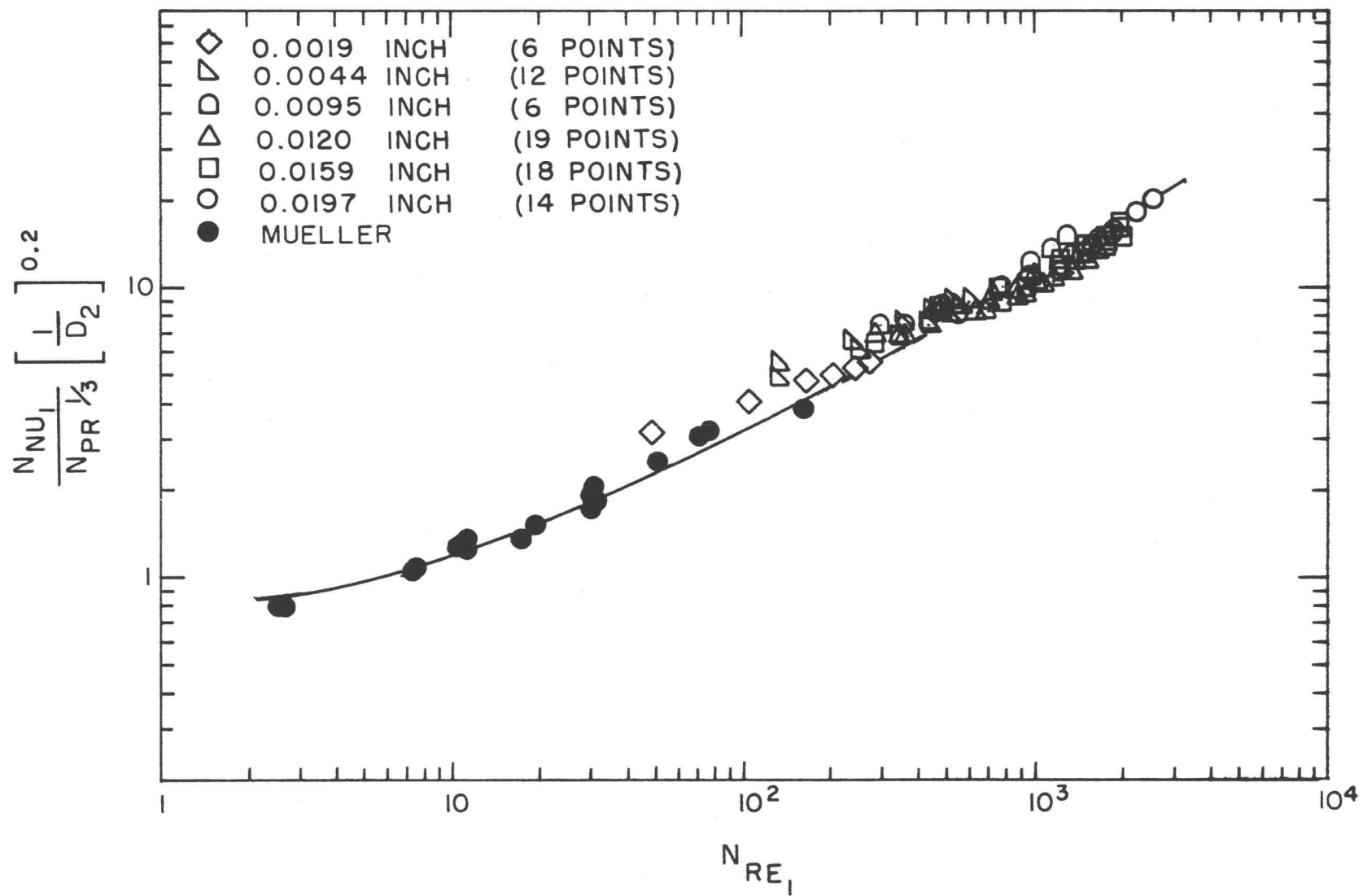


Figure 4. Correlation Based on Wire and Tube Diameters.

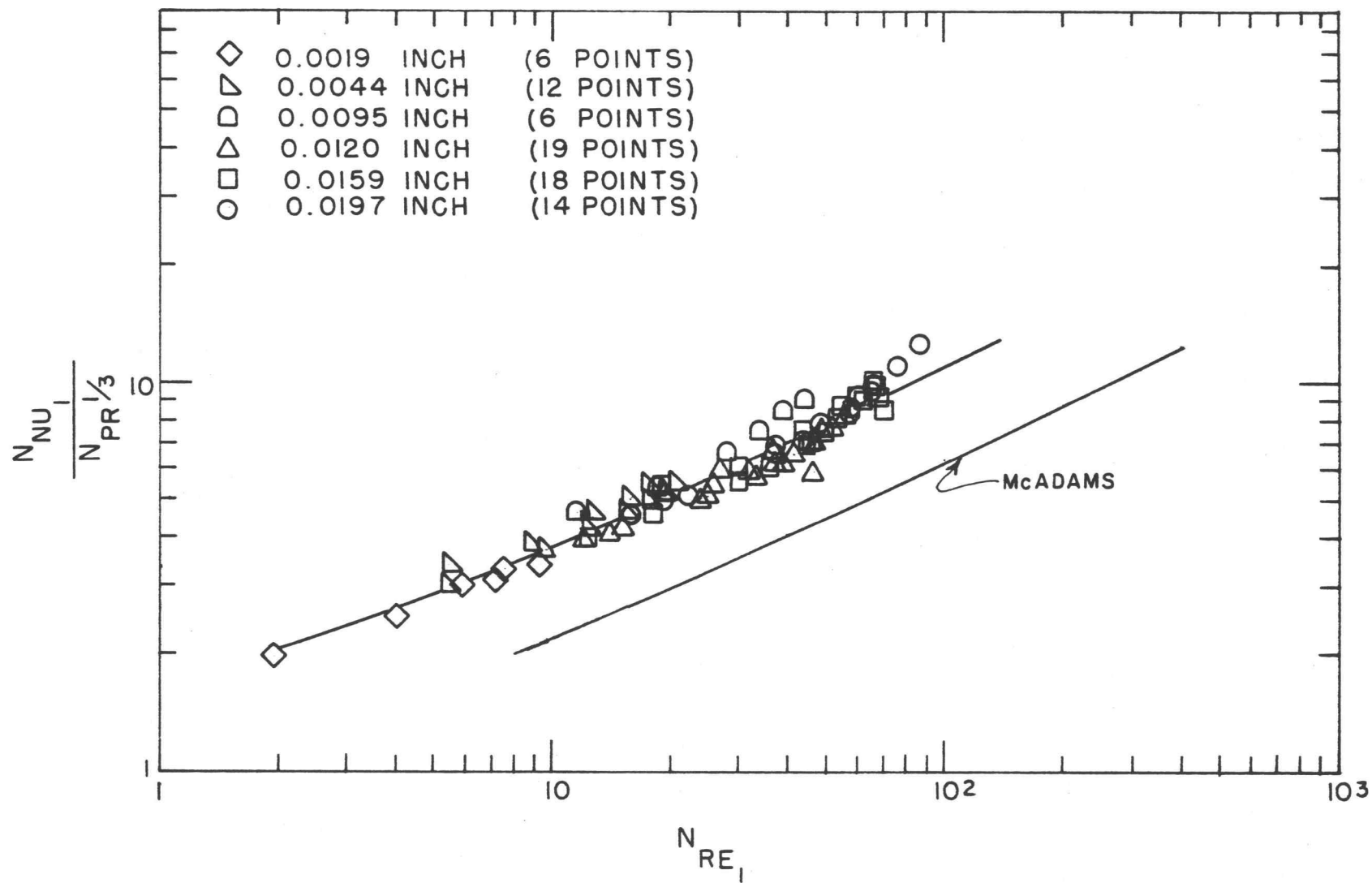


Figure 5. Correlation Based on Wire Diameter and Fluctuating Radial Velocity.

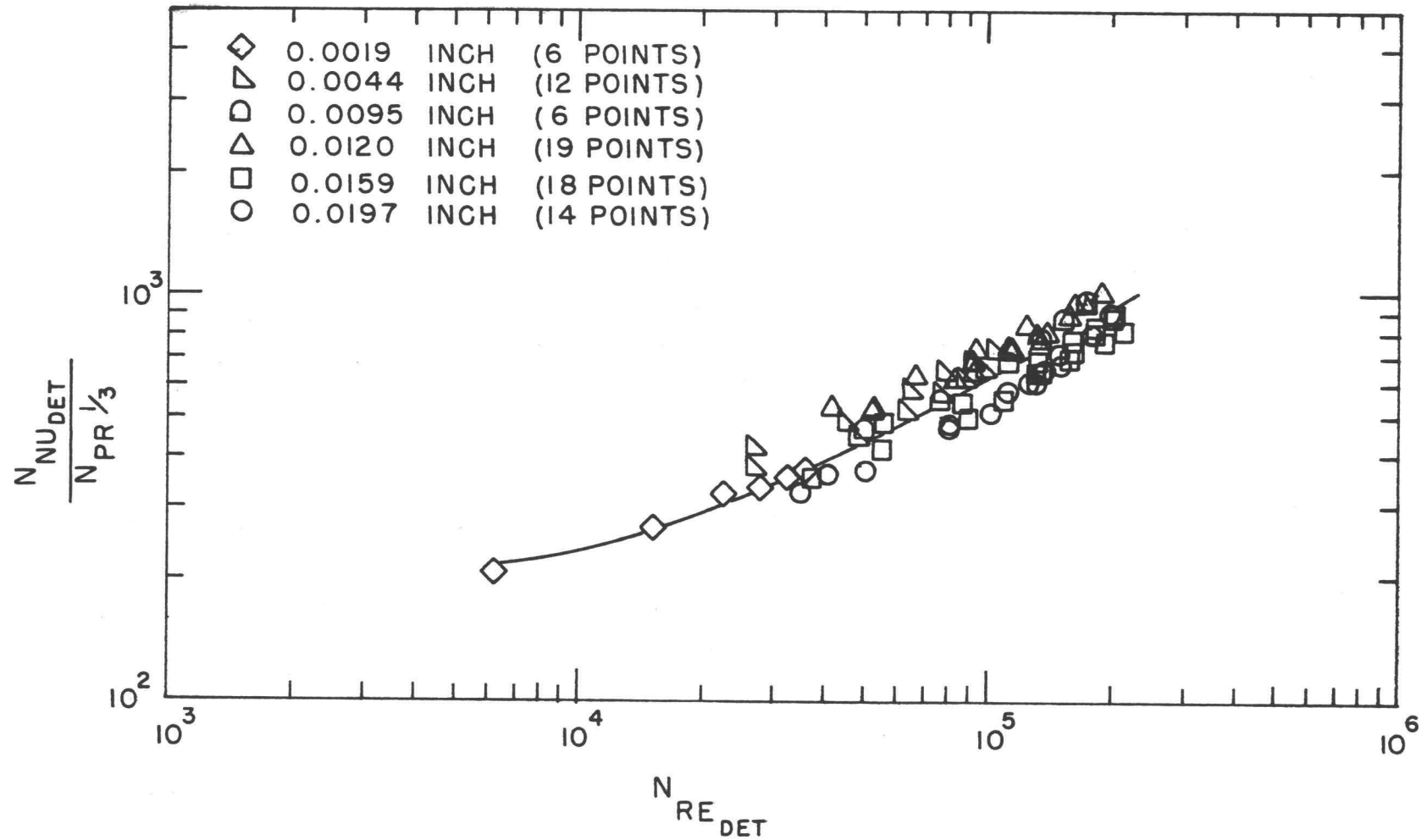


Figure 6. Correlation Based on Film Conditions and Equivalent Diameter for Turbulent Flow.

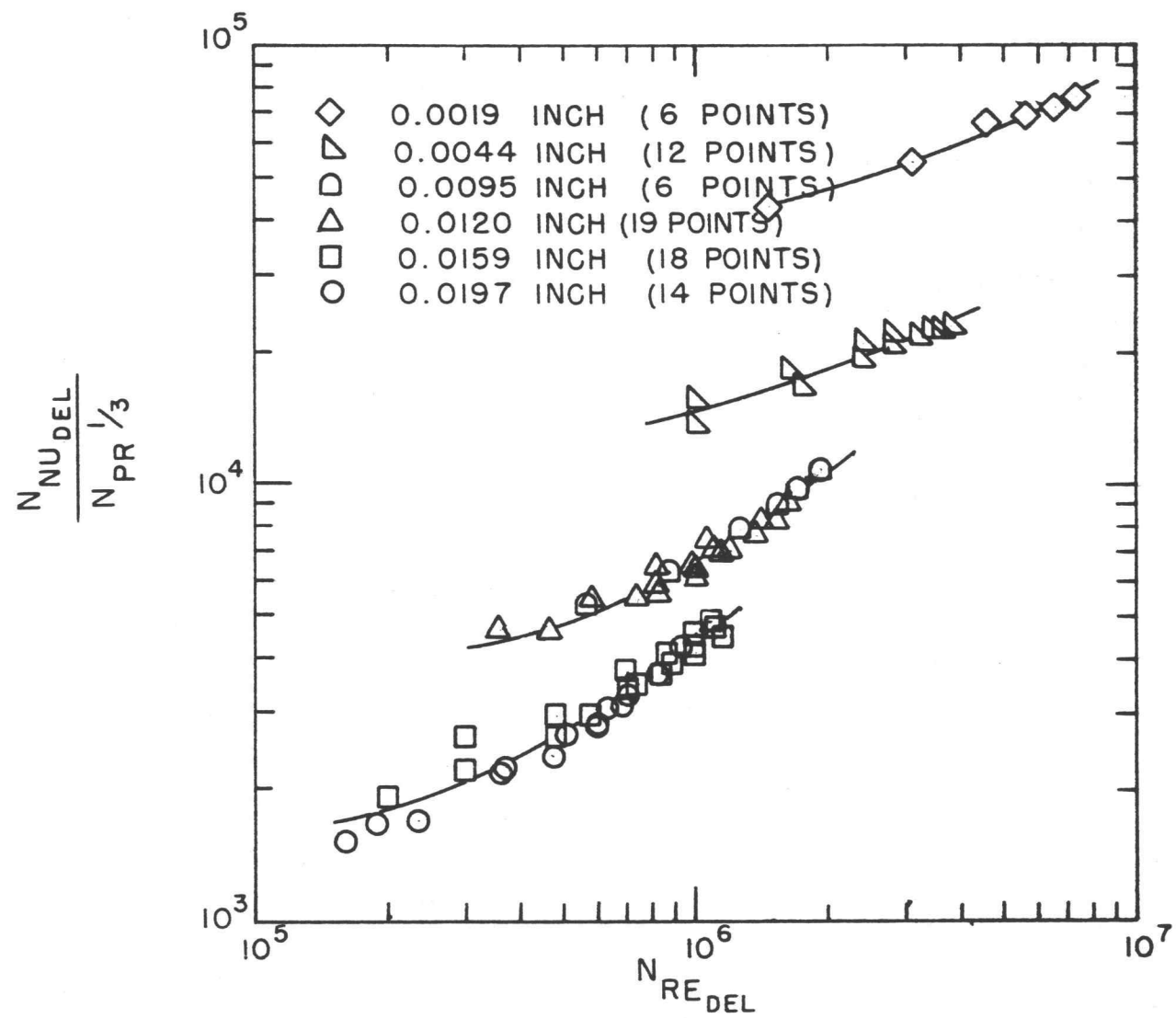


Figure 7. Correlation Based on Film Conditions and Equivalent Diameter For Laminar Flow.

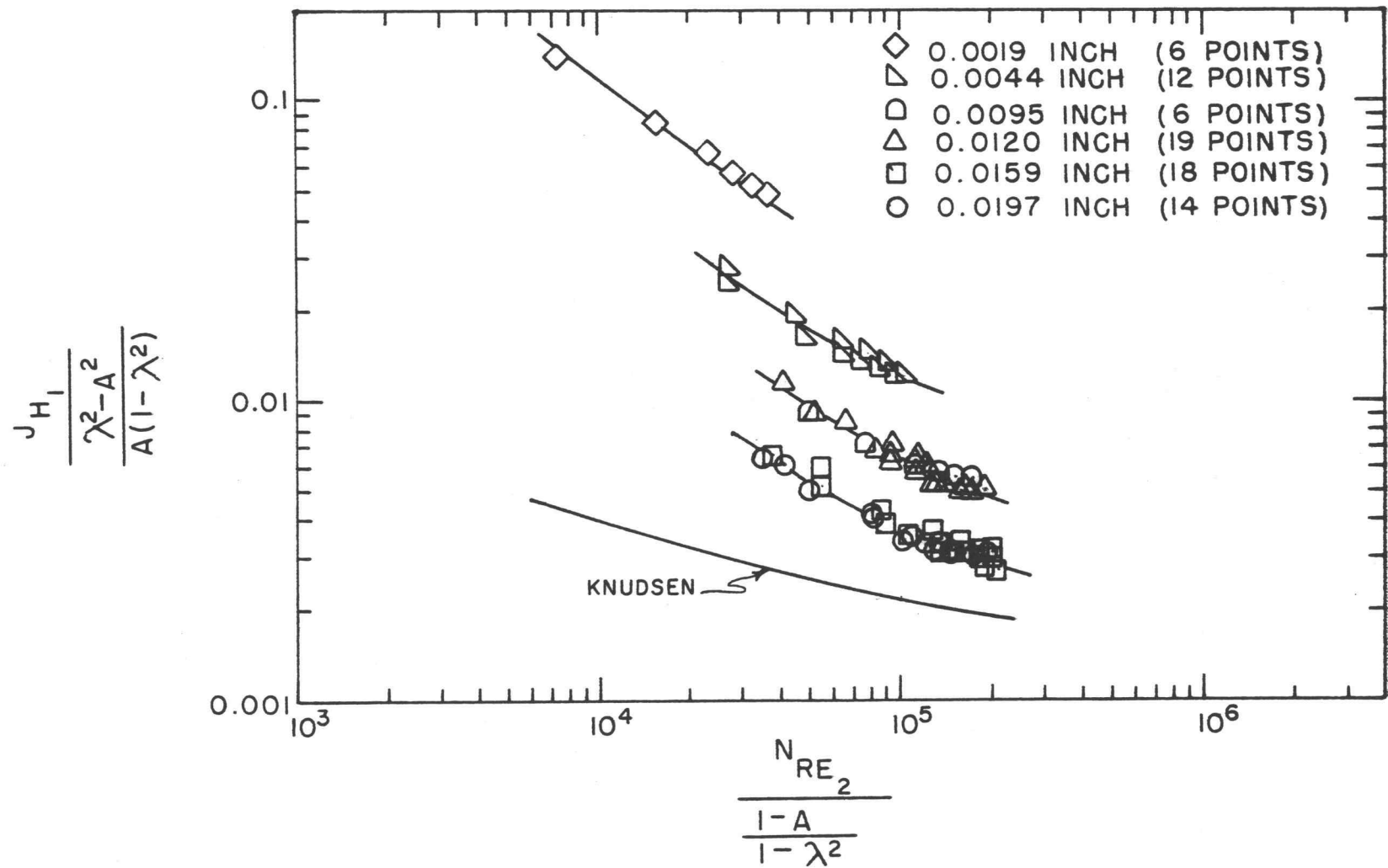


Figure 8. Correlation Based on Film Conditions and Equivalent Diameter For Turbulent Flow. 22

N_{Re_1} based on the fluctuating radial velocity v' . The fluctuating velocity was calculated at the axis of circular pipes from data by Laufer (5). Also presented is a plot of the equation recommended by McAdams (7) for flow transverse to cylinders.

Figures 6 and 7 present the data by plotting $N_{Nu_{det}}/N_{Pr}^{1/3}$ and $N_{Nu_{del}}/N_{Pr}^{1/3}$ versus $N_{Re_{det}}$ and $N_{Re_{del}}$, respectively. Det was calculated using the point of maximum turbulent velocity as determined experimentally in annuli by Brighton and Jones (1). At the diameter ratios used in the present study, a similar plot would have been obtained using the point of maximum turbulent velocity predicted analytically for annuli by Macagno and McDougall (6). Del was calculated using the point of maximum laminar velocity as shown analytically by Knudsen and Katz (4).

$$r_m = \left[\frac{r_2^2 - r_1^2}{2 \ln \frac{r_2}{r_1}} \right]^{0.5}$$

In Figure 8, $j_{h_1} / \frac{\lambda^2 - A^2}{A(1 - \lambda^2)}$ is plotted versus $N_{Re_2} / \frac{1 - A}{1 - \lambda^2}$. The r_m used in evaluating λ was obtained from the work of Brighton and Jones (1) and is therefore a point of maximum turbulent velocity rather than a point of maximum turbulent velocity originally presented by Knudsen (3). The curve recommended by Knudsen is also shown.

DISCUSSION

As shown in Figure 3, the present data correlated well when plotted in a manner similar to that used by Mueller (9) but with an adjustment for the variation in N_{Pr} . The variation in N_{Pr} must be considered if Mueller's method is to be applicable for fluids other than air.

The present data and that of Mueller (9) compared well when plotted in Figure 4. For the purpose of comparing data, N_{Pr} for air was assigned a value of 0.72 since it varies little over a wide temperature range and because insufficient information was presented in Mueller's paper to determine correct values.

Because Mueller's correlation and the usual empirical equations differ in the method of describing the geometry of the system it is not possible to predict whether Mueller's correlation will be satisfactory for annuli of diameter ratios less than 50.

It is interesting to note that the slope of the curve in Figure 3 is about 0.5, the same as obtained for fluid flow transverse to cylinders.

To further investigate the latter point, the data were plotted in Figure 5 along with McAdams' (7) recommended curve for flow transverse to cylinders. No attempt was made to determine the radial fluctuating velocity necessary to obtain coincidence with McAdams'

curve. Rather, the ratio of the root mean square velocity fluctuation to the friction velocity (u^*) at the axis of a pipe as determined experimentally with air by Laufer (5) was used. The data and recommended curve have a similar slope which could indicate that, by actual measurement of radial fluctuating velocity at Reynold's numbers comparable to those used in the present study, a satisfactory correlation might result. Comparing the recommended curve to the data in Figure 3 reveals that a fluctuating cross velocity of about ten percent of the main stream velocity would result in good agreement of the present data with McAdams' curve.

Figures 6 and 7 show the results when the equivalent diameter is based on experimentally determined points of maximum turbulent velocity and on points of maximum laminar velocity respectively. The largest diameter ratio used by Brighton and Jones (1) was 16. It was therefore necessary to extrapolate their data to zero in order to obtain the r_m used in the calculations. A better correlation might have resulted if experimental data were available on the point of maximum turbulent velocity in annuli at large diameter ratios.

Figure 8 reveals an apparent diameter effect when the data is plotted as recommended by Knudsen (3) even though the experimentally determined value of the point of maximum velocity was used in calculationg λ .

Table 1 shows measured coefficients for the 0.0019-inch wire

compared with those predicted by Wiegand (12), Monrad and Pelton (8), and Knudsen (3). The measured coefficients are all below predicted values. They are as low as one-tenth the value predicted by Knudsen's equations indicating that the approach used by Knudsen is not valid for annuli of the diameter ratio studied here. Likewise, other empirical equations are not applicable to the diameter ratio studied here.

CONCLUSIONS AND RECOMMENDATIONS

Although satisfactory methods for predicting heat transfer coefficients at the inner wall of annuli of large diameter ratio are presented, no method is currently available which is satisfactory over all ratios from one to infinity.

The use of fluctuating radial velocities in correlating heat transfer data in annuli of large diameter appears feasible, but additional experimental work is required. The use of fluctuating velocities at low diameter ratios would appear to hold little promise of success since in these cases the significant velocity is parallel to the annulus axis according to the usual empirical correlation.

The present data correlated best when Mueller's method (9) was used. Good correlation was obtained when the equivalent diameter was based on the experimentally determined radius of maximum velocity in turbulent annular flow.

Further work should be directed toward attempting to correlate available annular heat transfer data using Mueller's method and the radius of maximum velocity in turbulent annular flow. If the latter method looks promising, additional experimental work should be performed to determine turbulent velocity profiles in annuli of large and small diameter ratios.

1. Brighton, J. A. and J. B. Jones. Fully developed turbulent flow in annuli. *Journal of Basic Engineering* Ser. D, 86:835-844. December 1964.
2. Colburn, A. P. A method of correlating forced convection heat transfer data and a comparison with fluid friction. *Transactions of the American Institute of Chemical Engineers* 29: 174-210. 1933.
3. Knudsen, J. G. Note on j factors for turbulent flow in annuli. *Journal of the American Institute of Chemical Engineers* 8:565-568. 1962.
4. Knudsen, James G. and Donald L. Katz. *Fluid dynamics and heat transfer*. New York, McGraw-Hill, 1958. 576 p.
5. Laufer, John. The structure of turbulence in fully developed pipe flow. Washington, D. C., 1954. 18 p. (National Advisory Committee on Aeronautics. Report no. 1174)
6. Macagno, E. O. and David W. McDougall. Turbulent flow in annular pipes. *Journal of the American Institute of Chemical Engineers* 12:437-444. 1966.
7. McAdams, William H. *Heat transmission*. 3d ed. New York, McGraw-Hill, 1954. 532 p.
8. Monrad, C. C. and J. F. Pelton. Heat transfer by convection in annular spaces. *Transactions of the American Institute of Chemical Engineers* 38:596-611. 1942.
9. Mueller, A. C. Heat transfer from wires to air. *Transactions of the American Institute of Chemical Engineers* 38:613-629. 1942.
10. Nolan, Lawrence Lyle. Incipient boiling and burnout heat flux for subcooled water flowing in annuli containing heated concentric wires. Master's thesis. Corvallis, Oregon State University, 1965. 38 numb. leaves.
11. Rothfus, R. R., C. C. Monrad, K. G. Sikchi, and W. J. Heideger. Isothermal skin friction in flow through annular sections. *Industrial and Engineering Chemistry*, 47:913-918. 1955.
12. Wiegand, J. H. Discussion of paper by McMillen and Larson. *Transactions of the American Institute of Chemical Engineers*. 41:147-152. 1945.

APPENDIX

APPENDIX I

NOMENCLATURE

| <u>Symbol</u> | <u>Definition</u> | <u>Units</u> |
|---------------|---|--|
| A | diameter ratio d_1/d_2 | |
| A_1 | wire surface area | ft^2 |
| A_2 | tube area | ft^2 |
| C_p | heat capacity at constant pressure | $\frac{\text{BTU}}{\text{LBM} \cdot ^\circ\text{F}}$ |
| d | diameter | ft |
| de | equivalent diameter, $d_e = d_2 - d_1$ | ft |
| del | equivalent diameter based on laminar flow maximum velocity radius | ft |
| dem | equivalent diameter based on the radius of maximum velocity. $d_{em} = 2r_1 \left[\left(\frac{r_m}{r_1} \right)^2 - 1 \right]$ | ft |
| det | equivalent diameter based on turbulent flow maximum velocity radius measured by Brighton and Jones (1). | ft |
| f | Fanning friction factor | |
| G | mass velocity | $\frac{\text{LBM}}{\text{ft}^2 \cdot \text{sec.}}$ |
| \bar{h} | average heat transfer coefficient | $\frac{\text{BTU}}{\text{hr. ft.}^2 \cdot ^\circ\text{F}}$ |
| j_h | j factor for heat transfer | |
| k | thermal conductivity | $\frac{\text{BTU}}{\text{hr. ft.} \cdot ^\circ\text{F}}$ |
| N_{Nu} | Nusselt number, $\frac{\bar{h}d}{k}$ | |

| | | |
|-------------|---|--------|
| N_{Pr} | Prandtl number, $\frac{C_p \mu}{k}$ | |
| r_m | radius at point of maximum velocity | ft |
| r_{ml} | radius at maximum velocity for laminar flow | |
| | $r_{ml}^2 = \frac{r_2^2 - r_1^2}{2 \ln \frac{r_2}{r_1}}$ | ft |
| N_{Re} | Reynold's number, $\frac{DG}{\mu}$ | |
| $N_{Re_v'}$ | Reynold's number based on fluctuating radial velocity | |
| R_I | current shunt resistance | ohms |
| R_s | standard resistance | ohms |
| R_v | variable resistance | ohms |
| R_w | test wire resistance | ohms |
| R_{ws} | test wire shunt resistance | ohms |
| T_B | bulk fluid temperature | °F |
| T_w | wire temperature | °F |
| U | bulk average fluid velocity | ft/sec |
| u^* | friction velocity, $u^* = U \left(\frac{f}{2} \right)^{0.5}$ | ft/sec |
| v' | fluctuating radial velocity | ft/sec |

Greek Letters

| | | |
|-----------|--------------------------|---------------------|
| λ | radius ratios, r_m/r_2 | |
| ρ | density | LBM/ft ³ |
| μ | dynamic viscosity | LBM/ft sec |

Subscripts

| | |
|---|------------------------------------|
| 1 | refers to wire |
| 2 | refers to tube |
| f | arithmetic average film conditions |
| w | wall conditions |
| b | bulk conditions |

APPENDIX II

EXPERIMENTAL DATA

Appendix Table 1. Summary of experimental data, 0.0019 inch wire

| A_1 | Amperes | R_w | T_w | T_b | \bar{E} | $\rho A_2 U$ |
|----------|---------|-------|-------|-------|-----------|--------------|
| 0.000891 | 2.12 | 20.88 | 129.5 | 79.7 | 7210 | 1.0 |
| | 2.17 | 20.32 | 119.0 | 79.1 | 9190 | 2.2 |
| | 2.21 | 19.91 | 111.5 | 78.3 | 11200 | 3.5 |
| | 2.22 | 19.81 | 109.8 | 77.8 | 11690 | 4.3 |
| | 2.22 | 19.67 | 107.2 | 77.2 | 12386 | 5.1 |
| | 2.23 | 19.55 | 105.0 | 76.4 | 13020 | 5.8 |

Appendix Table 2. Summary of experimental data, 0.0044 inch wire

| A_1 | Amperes | R_w | T_w | T_b | \bar{E} | $\rho A_2 U$ |
|---------|---------|-------|-------|-------|-----------|--------------|
| 0.00212 | 6.750 | 5.225 | 114.3 | 71.9 | 9630 | 5.9 |
| | 6.714 | 5.251 | 115.8 | 72.4 | 8780 | 5.18 |
| | 6.649 | 5.292 | 119.0 | 72.9 | 8170 | 4.37 |
| | 6.582 | 5.355 | 124.2 | 73.4 | 7350 | 3.48 |
| | 6.485 | 5.497 | 135.5 | 74.2 | 6070 | 2.25 |
| | 6.356 | 5.628 | 146.1 | 75.1 | 5150 | 1.27 |
| 0.00212 | 6.254 | 5.417 | 108.0 | 68.7 | 8667 | 5.83 |
| | 6.220 | 5.446 | 111.2 | 69.4 | 8117 | 5.16 |
| | 6.173 | 5.493 | 115.0 | 70.3 | 7540 | 4.35 |
| | 6.088 | 5.568 | 121.0 | 71.0 | 6646 | 3.40 |
| | 6.015 | 5.662 | 128.7 | 72.1 | 5828 | 2.53 |
| | 5.879 | 5.845 | 143.5 | 73.2 | 4627 | 1.30 |

Appendix Table 3. Summary of experimental data, 0.0095 inch wire

| A_1 | Amperes | R_w | T_w | T_b | \bar{n} | $\rho A_2 U$ |
|---------|---------|-------|-------|-------|-----------|--------------|
| 0.00465 | 18.16 | 0.972 | 105.5 | 71.9 | 7000 | 5.85 |
| | 17.98 | 0.980 | 109.0 | 72.4 | 6360 | 5.16 |
| | 18.01 | 0.988 | 114.5 | 73.0 | 5670 | 4.36 |
| | 17.83 | 1.008 | 121.5 | 73.7 | 4920 | 3.46 |
| | 17.62 | 1.041 | 136.0 | 74.5 | 3860 | 2.18 |
| | 17.41 | 1.072 | 149.7 | 75.4 | 3210 | 1.30 |

Appendix Table 4. Summary of experimental data, 0.012 inch wire

| A_1 | Amperes | R_w | T_w | T_b | E | $\rho A_2 U$ |
|---------|---------|--------|-------|-------|------|--------------|
| 0.00582 | 21.71 | 0.6762 | 120.5 | 69.2 | 3640 | 3.95 |
| | 21.68 | 0.6848 | 126.0 | 69.4 | 3340 | 3.30 |
| | 21.52 | 0.6983 | 134.5 | 70.0 | 2900 | 2.53 |
| | 21.12 | 0.7299 | 154.8 | 71.5 | 2290 | 1.27 |
| 0.00568 | 21.22 | 0.7044 | 156.1 | 73.0 | 2300 | 1.01 |
| | 21.74 | 0.6597 | 131.6 | 70.7 | 3100 | 2.55 |
| | 21.86 | 0.6464 | 124.2 | 69.8 | 3400 | 3.25 |
| | 21.86 | 0.6414 | 119.0 | 69.2 | 3700 | 3.90 |
| 0.00580 | 21.75 | 0.6562 | 109.5 | 72.1 | 4880 | 5.83 |
| | 21.77 | 0.6643 | 114.7 | 73.2 | 4460 | 4.93 |
| | 21.74 | 0.6712 | 119.0 | 71.7 | 3950 | 3.63 |
| | 21.59 | 0.6847 | 127.5 | 71.4 | 3370 | 2.62 |
| | 21.34 | 0.7049 | 139.9 | 72.4 | 2800 | 1.73 |
| 0.00580 | 21.42 | 0.6309 | 103.0 | 66.3 | 4640 | 5.80 |
| | 21.18 | 0.6376 | 107.3 | 67.7 | 4250 | 5.10 |
| | 21.06 | 0.6436 | 111.0 | 67.8 | 3890 | 4.37 |
| | 20.96 | 0.6553 | 118.2 | 68.6 | 3420 | 3.47 |
| | 20.68 | 0.6755 | 128.0 | 69.3 | 2880 | 2.37 |
| | 20.43 | 0.7014 | 144.0 | 70.4 | 2330 | 1.34 |

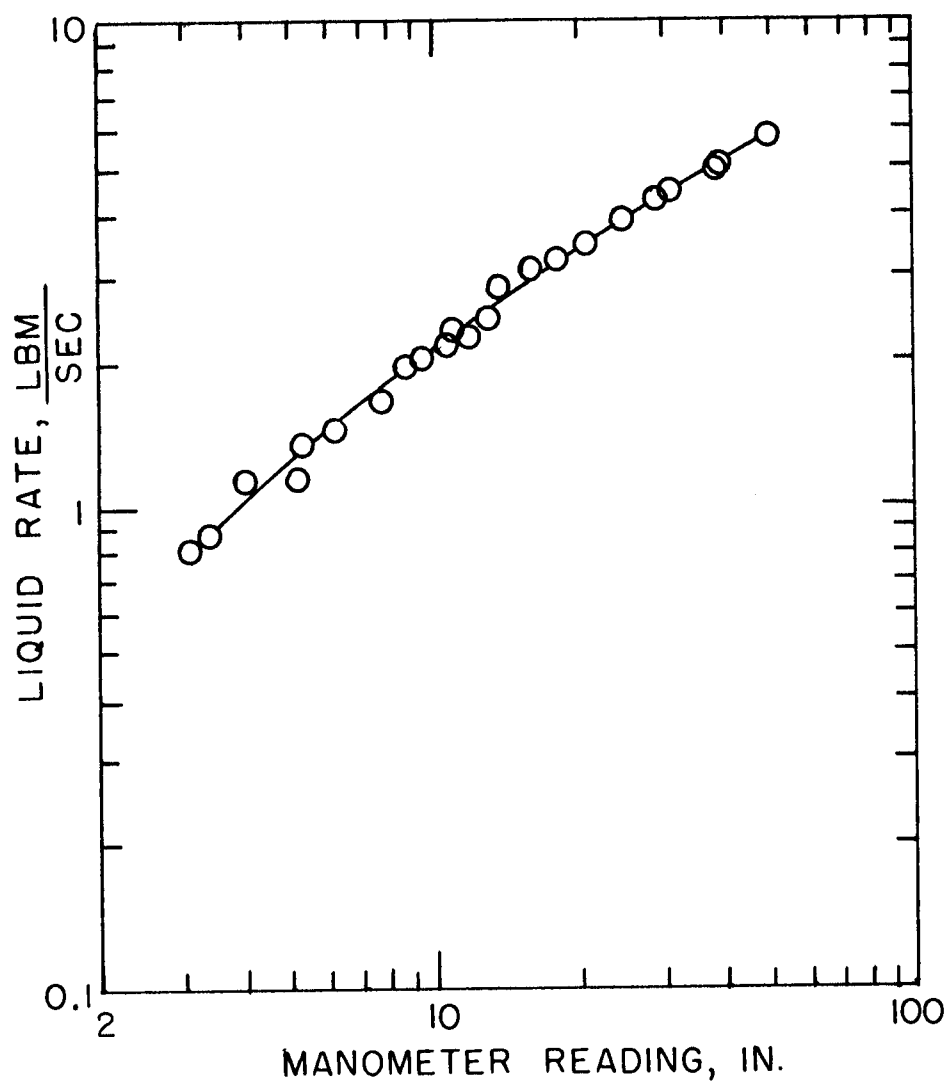
Appendix Table 5. Summary of experimental data, 0.0159 inch wire

| A_1 | Amperes | R_w | T_w | T_b | \bar{h} | $\rho A_2 U$ |
|---------|---------|--------|-------|-------|-----------|--------------|
| 0.00771 | 25.18 | 0.3818 | 100.2 | 69.8 | 3540 | 4.06 |
| | 25.01 | 0.3893 | 108.0 | 70.4 | 2810 | 2.67 |
| | 25.08 | 0.3834 | 101.9 | 69.6 | 3300 | 3.49 |
| | 24.67 | 0.4047 | 124.1 | 70.9 | 2050 | 1.22 |
| | 25.11 | 0.3761 | 93.8 | 67.8 | 4040 | 5.18 |
| | 25.47 | 0.3740 | 91.5 | 66.9 | 4370 | 5.80 |
| 0.00771 | 25.31 | 0.3692 | 88.4 | 66.0 | 4700 | 5.80 |
| | 25.33 | 0.3733 | 91.5 | 66.7 | 4300 | 5.15 |
| | 25.16 | 0.3779 | 96.3 | 68.2 | 3800 | 4.55 |
| | 25.02 | 0.3825 | 101.1 | 69.0 | 3300 | 3.47 |
| | 24.93 | 0.3933 | 112.4 | 69.8 | 2500 | 2.15 |
| | 24.55 | 0.4177 | 137.0 | 72.2 | 1700 | 0.77 |
| 0.00771 | 25.34 | 0.3690 | 87.3 | 65.4 | 4790 | 5.80 |
| | 25.27 | 0.3719 | 90.2 | 66.6 | 4420 | 5.10 |
| | 25.15 | 0.3754 | 93.8 | 67.8 | 4040 | 4.55 |
| | 25.12 | 0.3797 | 98.3 | 68.6 | 3570 | 3.41 |
| | 24.95 | 0.3889 | 107.9 | 69.7 | 2810 | 2.17 |
| | 24.94 | 0.3981 | 116.1 | 71.0 | 2430 | 1.30 |

Appendix Table 6. Summary of experimental data, 0.0197 inch wire

| A_1 | Amperes | R_w | T_w | T_b | \bar{h} | $\rho A_2 U$ |
|---------|---------|--------|-------|-------|-----------|--------------|
| 0.00956 | 26.82 | 0.2248 | 91.9 | 73.6 | 3440 | 3.60 |
| | 26.92 | 0.2471 | 95.6 | 74.0 | 2960 | 2.83 |
| | 27.02 | 0.2505 | 100.4 | 74.7 | 2540 | 2.04 |
| | 27.12 | 0.2547 | 106.7 | 70.4 | 1840 | 1.01 |
| 0.00975 | 27.20 | 0.2447 | 86.2 | 68.8 | 3640 | 4.18 |
| | 27.17 | 0.2465 | 88.8 | 69.2 | 3280 | 3.57 |
| | 27.15 | 0.2498 | 93.8 | 69.8 | 2690 | 2.72 |
| | 27.08 | 0.2581 | 107.4 | 71.4 | 1890 | 1.22 |
| 0.00961 | 27.46 | 0.2387 | 80.0 | 67.2 | 4990 | 5.80 |
| | 27.44 | 0.2409 | 83.8 | 68.8 | 4290 | 5.03 |
| | 27.55 | 0.2432 | 87.4 | 70.0 | 3770 | 4.12 |
| | 27.47 | 0.2456 | 91.3 | 70.9 | 3220 | 3.43 |
| | 27.47 | 0.2510 | 99.9 | 72.4 | 2450 | 2.03 |
| | 27.21 | 0.2607 | 115.6 | 73.8 | 1640 | 0.79 |

APPENDIX III



Appendix Figure 1. Orifice Calibration.

APPENDIX IV

SAMPLE CALCULATIONS

0.0019 Inch Diameter Wire

1. \bar{h}

$$\bar{h} = \frac{q}{A_1(T_w - T_b)} = \frac{3.414 I^2 R_w}{A_1(T_w - T_b)}$$

$$\bar{h} = \frac{(3.414)(2.12)^2(20.88)}{(8.91 \times 10^{-4})(129.5 - 79.7)} = 7210$$

2. N_{Re_1}

$$N_{Re_1} = (\rho A_2 U) \frac{D_1}{\mu A_2} = \frac{(1.0)(0.0019)(4)(144)}{(12)(0.58 \times 10^{-3})(3.14)(1.01)^2} = 48.8$$

3. $N_{Re_{v'}}$

$$N_{Re_{v'}} = \frac{\rho d_1 \sqrt{v'^2}}{\mu}$$

From data by Rothfus, et. al. (11), at the center of a pipe

$$\frac{\sqrt{v'^2}}{U^*} = 0.75$$

$$U^* = U \sqrt{\frac{f}{2}}$$

$$\frac{1}{\sqrt{f}} = 4.0 \log N_{Re_2} \sqrt{f} - 0.40$$

$$N_{Re_2} = (\rho A_2 U) \frac{D_2}{A_2 \mu}$$

$$N_{Re_2} = \frac{(1.0)(1.01)(4)(144)}{(12)(3.14)(1.01)^2(0.58 \times 10^{-3})} = 26000$$

$$\sqrt{\frac{f}{2}} = 0.054$$

$$U = \frac{(\rho A_2 U)}{\rho A_2} = \frac{(1.0)(144)(4)}{(62.4)(3.14)(1.01)^2} = 2.88$$

$$U^* = (2.88)(0.054) = 0.156$$

$$\sqrt{\bar{v}'^2} = (0.156)(0.75) = 0.117$$

$$N_{Re_{v'}} = \frac{(62.4)(0.0019)(0.117)}{0.58 \times 10^{-3}} = 1.99$$

$$4. \quad N_{Re_{det}} = \frac{\rho U_{det}}{\mu_f}$$

From Brighton and Jones (1)

$$\text{At } \frac{D_1}{D_2} = \frac{0.0019}{1.01} = 0.00188, \quad \frac{r_m}{r_2} = 0.02$$

$$r_m = \left(\frac{1.01}{2}\right)(0.02) = 0.0101 \text{ inch}$$

$$\det = 2r_1 \left[\left(\frac{r_m}{r_1} \right)^2 - 1 \right]$$

$$\text{det} = 0.0019 \left[\left(\frac{0.0101}{0.00095} \right)^2 - 1 \right] = 0.213 \text{ inch}$$

$$N_{\text{Re}_{\text{det}}} = \frac{(62.4)(2.88)(0.213)}{(0.44 \times 10^{-3})(12)} = 7300$$

5. $N_{\text{Re}_{\text{del}}}$

$$N_{\text{Re}_{\text{del}}} = \frac{\rho U_{\text{del}}}{\mu_f}$$

$$\text{del} = 2r_1 \left[\left(\frac{r_m}{r_1} \right)^2 - 1 \right]$$

$$r_m = \left[\frac{r_2^2 - r_1^2}{2 \ln \left(\frac{r_2}{r_1} \right)} \right]^{0.5}$$

$$r_m = \left[\frac{(0.505)^2 - (0.00095)^2}{2 \ln \frac{0.505}{0.00095}} \right]^{0.5} = 0.142 \text{ inch}$$

$$\text{del} = 0.0019 \left[\left(\frac{0.142}{0.00095} \right)^2 - 1 \right] = 42.7 \text{ inches}$$

$$N_{\text{Re}_{\text{del}}} = \frac{(62.4)(2.88)(42.7)}{(0.44 \times 10^{-3})(12)} = 1.45 \times 10^6$$

6. $\frac{1 - A}{1 - \lambda^2}$

$$A = \frac{r_1}{r_2} = \frac{0.00095}{0.505} = 0.00188$$

$$\lambda = \frac{r_m}{r_2} = \frac{0.0101}{0.505} = 0.020$$

$$\frac{1-A}{1-\lambda^2} = \frac{0.998}{0.999} = 0.998$$

$$7. \quad \frac{\lambda^2 - A^2}{A(1-\lambda^2)}$$

$$\frac{\lambda^2 - A^2}{A(1-\lambda^2)} = \frac{0.0004}{(0.00188)(0.999)} = 0.211$$

$$8. \quad j_{h_1}$$

$$j_{h_1} = \frac{\bar{H}_1}{C_p G} (N_{Pr_f})^{2/3} = \frac{(7210)(4.35)^{2/3}}{(1.0)(180)(3600)} = 0.0297$$